[CANCER RESEARCH 59, 1202–1205, March 15, 1999]

*Advances in Brief*

# Correlation of β-Actin Messenger RNA Localization with Metastatic Potential in Rat Adenocarcinoma Cell Lines[1]

**Elena A. Shestakova, Jeffrey Wyckoff, Joan Jones, Robert H. Singer, and John Condeelis[2]**

*Departments of Anatomy and Structural Biology [E. A. S., J. W., R. H. S., J. C.] and Pathology [J. J.], Albert Einstein College of Medicine, Bronx, New York 10461*

## Abstract

**The actin cytoskeleton is involved in the motility of tumor cells. It has been shown in several cell types that β-actin mRNA is localized in the protrusions of cells in which actin is actively polymerized, and the ability to localize mRNA is correlated with the efficiency of motility. In this context, we studied the distribution of β-actin mRNA in two different tumor cell lines and correlated it with their metastatic potential. The two cell lines used were the highly metastatic MTLn3 cells and nonmetastatic MTC cells. Nonmetastatic MTC cells have two different pools of β-actin mRNA (perinuclear and at the leading edge), whereas highly metastatic MTLn3 cells have only a perinuclear distribution of β-actin mRNA. These differences in mRNA localization are correlated with profound differences in the polarity and plasticity of cell motility of these cells in culture and the histopathology of primary breast tumors derived from these cells. In particular, MTLn3 cells are unpolarized by all cell shape and motility criteria in culture and in their histopathological organization in primary tumors. By comparison, MTC cells are polarized in all identical measurements. These results suggest that the increased plasticity of cell locomotion and the invasiveness of MTLn3 cells result from the failure of metastatic cells to localize β-actin mRNA properly, causing them to be less polarized and therefore more flexible in their direction of motility. Thus, differences in the polarized organization of cells in the primary tumor that are correlated with β-actin mRNA localization may have prognostic value in predicting metastatic potential.**

## Introduction

The metastatic process may involve chemotaxis of a subpopulation of tumor cells (1, 2). Highly metastatic cells exhibit highly plastic cell motility and true chemotaxis to EGF[3] (3). The chemotactic response involves the formation of cellular protrusions in response to chemoattractant, and these protrusions contain newly polymerized actin filaments (3, 4). Actin filament formation in cellular protrusions has been extensively studied. EGF-stimulated nucleation sites under the plasma membrane lead to a local net increase in actin polymerization that is proposed to provide the force for lamellipod extension (3, 4). The location of these nucleation sites establishes the direction of cell movement. However, it is still unclear whether actin monomers diffuse to the sites of actin filament formation or whether locally synthesized G-actin represents the population of actin monomers that polymerize into the filaments at the leading edge.

It has been shown previously that β-actin mRNA is localized in protrusions in several normal cell types (5–8) and that β-actin is preferentially polymerized at the leading lamella (9). *Cis*-acting elements responsible for the localization of β-actin mRNA were found in the 3′-UTR (8). The 54 nucleotides 3′ of the stop codon were the most potent in localizing mRNA and were named the zip code. A protein of $M_r$ 68,000 named zip code-binding protein was found that binds the zip code in β-actin mRNA. Binding was correlated with the localization of β-actin mRNA (10).

It was proposed that β-actin translated from localized mRNA could incorporate into filaments, endowing them with the ability to interact with specific actin-binding proteins [for example, β-actin filament-specific ezrin and β-CAP73 (11, 12)], thereby leading to the establishment of cell polarity.

In relation to this, the present study was undertaken to determine the localization of β-actin mRNA in two well-characterized types of cancer cell lines, MTC and MTLn3 cells derived from a rat mammary adenocarcinoma (13, 14). These cell lines have different metastatic potential and actin cytoskeleton organization. MTLn3 cells are highly metastatic, and they contain comparatively small amounts of F-actin in the leading edge, whereas MTC cells are nonmetastatic and have a well-developed leading edge with a large amount of F-actin (2–4, 13–15). *In situ* hybridization was carried out to determine the extent to which β-actin mRNA becomes localized in these two different cell types under different culture conditions and whether this is correlated with the type of cell motility observed *in vitro* and the structure of the tumor cells within the primary tumor both *in vivo* and *in situ.*

## Materials and Methods

**Cell Culture.** Rat mammary adenocarcinoma MTLn3 and MTC cell lines were used in this study. Their metastatic potentials (high metastatic potential, for MTLn3 cell line; low metastatic potential, MTC cell line) have been described previously (13, 14). Cells were maintained in α-modified MEM (Life Technologies, Inc.) containing 5% fetal bovine serum and antibiotics (penicillin and streptomycin). Cells were cultivated on glass coverslips coated with 27 μg/ml rat tail collagen I (Collaborative Biochemicals). MTLn3 and MTC cells were starved by removing complete medium and incubating in α-modified MEM containing 10 mM HEPES, (pH 7.4) and 0.35% BSA for 3 h. The cells were then stimulated with complete α-modified MEM containing 5% fetal bovine serum. Cells were fixed at 37°C in 4% paraformaldehyde in PBS [1 mM $KH_2PO_4$, 10 mM $Na_2HPO_4$, 137 mM NaCl, and 2.7 mM KCl (pH 7.0)], washed in PBS, and dehydrated in 70% ethanol at 4°C overnight.

***In Situ* Hybridization.** Rat β-actin specific 3′-UTR probes and tubulin mRNA-specific probes were synthesized with amino linker on an Applied Biosystems 394 DNA/RNA synthesizer. β-actin 3′-UTR probes were labeled with CY3 (for protocols: http://singerlab.aecom.yu.edu). Tubulin mRNA-specific probes were digoxigenin labeled with terminal transferase. To detect β-actin mRNAs, 22-mm square coverslips were rehydrated in PBS, permealized with 0.5% Triton in PBS for 10 min, and then hybridized for 3 h at 37°C with 20 ng of a mixture of five oligonucleotides all capable of hybridizing with β-actin mRNA to increase the signal (~50 nucleotides each). Coverslips were washed twice with 50% formamide in 2× SSC [300 mM NaCl, and 30 mM sodium citrate (pH 7.0)], 2× SSC, and 1× SSC, and mounted. To detect tubulin mRNAs, coverslips were treated with oligonucleotide probes in the same way as for β-actin mRNA detection, and then, after extensive washing with formamide, SSC, and PBS, coverslips were incubated with monoclonal anti-digoxigenin antibodies labeled with CY3, followed by antimouse CY3-labeled antibodies.

Received 1/4/99; accepted 2/1/99.

The costs of publication of this article were defrayed in part by the payment of page charges. This article must therefore be hereby marked *advertisement* in accordance with 18 U.S.C. Section 1734 solely to indicate this fact.

[1] Supported by grants from the NIH (to R. H. S. and J. C.).

[2] To whom requests for reprints should be addressed, at Department of Anatomy and Structural Biology, Albert Einstein College of Medicine, 1300 Morris Park Avenue, Bronx, NY 10461.

[3] The abbreviations used are: EGF, epidermal growth factor; UTR, untranslated region; EF, elongation factor; DIAS, Dynamic Image Analysis System.

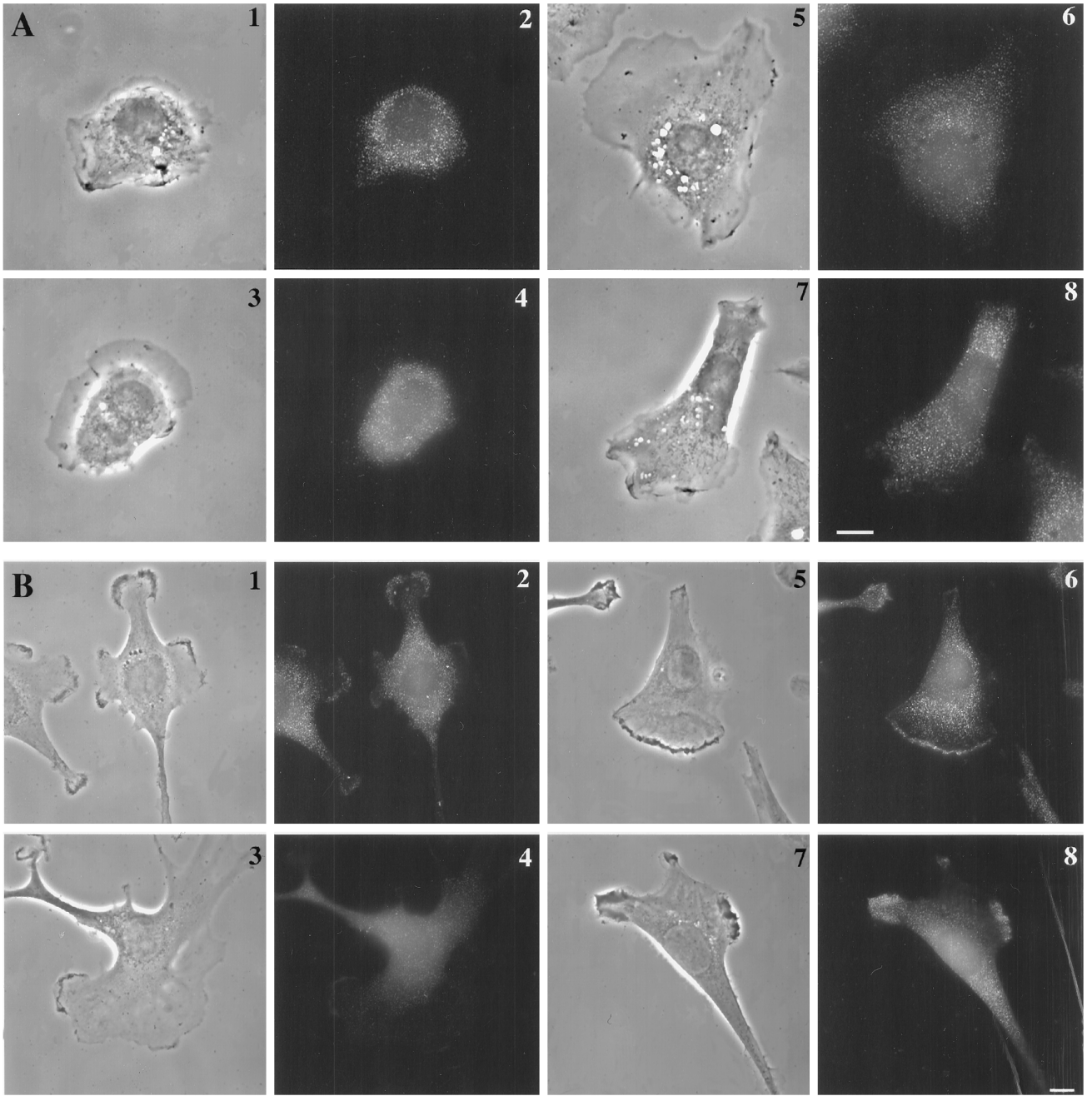


Fig. 1. β-actin mRNA localization in MTC and MTLn3 cells. *A*, MTLn3 cells. MTLn3 cells serum-starved for 3 hours (*1* and *2*); MTLn3 cells stimulated with 5% serum for 3 min (*3* and *4*), 10 min (*5* and *6*), and 30 min (*7* and *8*). *1, 3, 5,* and *7*, phase-contrast images of MTLn3 cells; *2, 4, 6,* and *8*, cells fluorescently labeled with rat β-actin mRNA-specific probes. *B*, MTC cells. *1* and *2*, cells grown continuously in serum. *3* and *4*, cells held in absence of serum for 3 h. *5–8*, MTC cells stimulated with 5% serum for 3 min. *1, 3, 5,* and *7*, phase-contrast images of MTC cells; *2, 4, 6,* and *8*, results of *in situ* hybridization with rat β-actin mRNA-specific probes. *Bar*, 10 μm.

Table 1 *Motility parameters of MTLn3 and MTC cell lines translocating in complete (+ serum) medium*

For all parameters, the total time interval was 15 min. The time interval between successive frames was 1 min. Differences in all presented parameters were statistically significant. SE, standard error. Parameters are defined as follows: net path length is the distance directly from the path starting point to the ending point; total path length is the sum of the lengths of the line segments connecting the centroids of the path; directionality is the net path length divided by the total path length; average instantaneous speed is an average of speed values at each time interval; average speed is the net path length divided by total time interval; and persistence is the speed divided by the change of direction given in grads.

| Cell type | Net path length (μm) | Total path length (μm) | Directionality (net/total) | Average instantaneous speed (μm/min) | Average speed (μm/min) | Persistence (μm/min × deg) |
|---|---|---|---|---|---|---|
| MTLn3 ($n$ = 21) | 5.39 | 20.41 | 0.27 | 0.97 | 0.39 | 0.21 |
| SE | 0.18 | 0.17 | 0.008 | 0.009 | 0.012 | 0.0036 |
| MTC ($n$ = 32) | 12.28 | 30.03 | 0.39 | 1.58 | 0.88 | 0.44 |
| SE | 0.29 | 0.28 | 0.0069 | 0.02 | 0.021 | 0.0084 |

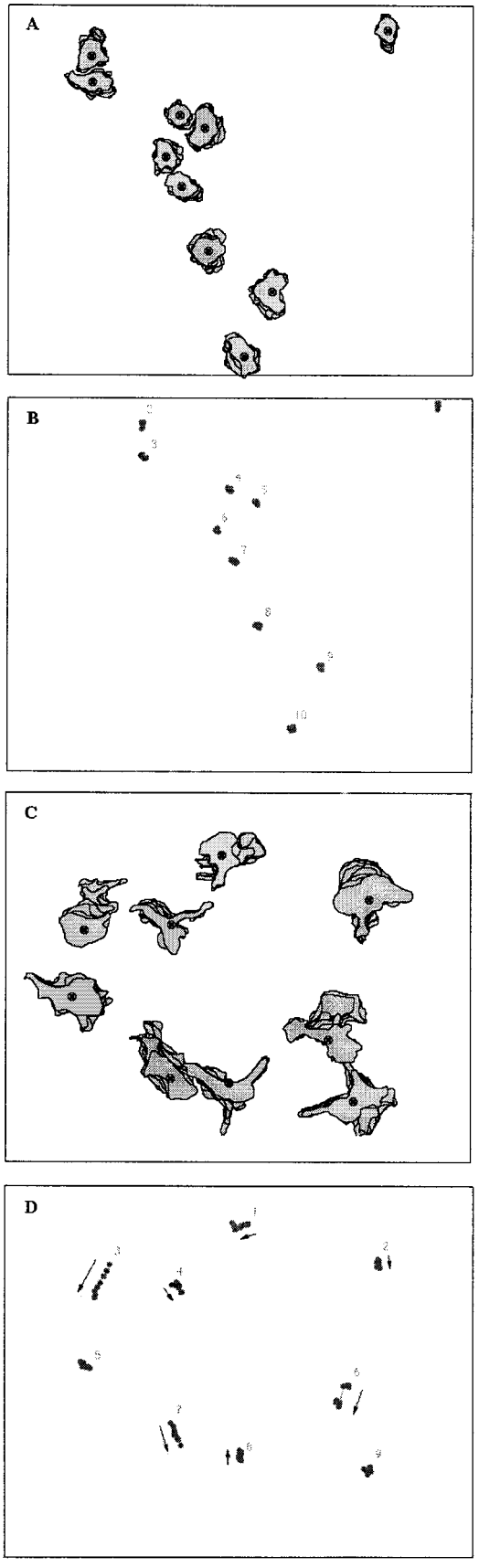


Fig. 2. Cell perimeter (*A* and *C*) and centroid (*B* and *D*) plots of 11 MTLn3 cells (*A* and *B*) and 9 MTC cells (*C* and *D*). For the centroid and perimeter tracks, the time interval between images was 2 min. Total time of movement was 15 min.

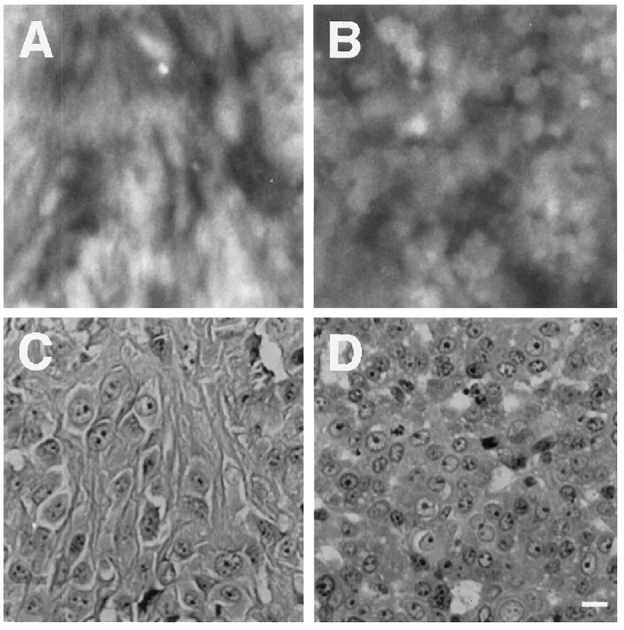


Fig. 3. Appearance of tumor cells *in vivo* and *in situ.* Mammary tumors were prepared by injecting green fluorescent protein-expressing MTC cells (*A*) or MTLn3 cells (*B*) into the mammary fat pad of rats and imaged in the primary tumor in live animals after 2.5 weeks of growth, as described previously (2). Identical tumors were imaged from H&E-stained paraffin sections of MTC (*C*) and MTLn3 (*D*) tumors. Note that MTC cells (*C*) have a more polarized epithelial pattern in primary tumors than MTLn3 cells. *Bar*, 20 μm.

**Computer-assisted Analysis of Cell Behavior.** Cells were recorded with a Nikon microscope equipped with a charge-coupled device camera through a ×10 objective with a 1-min time interval between image frames. Images were processed with DIAS software (16). Cell motility data were displayed as an overlay of cell perimeters as a stack of all time-lapsed images (cell perimeter plot) and as a centroid plot showing the location of the geometrical center of the cell as a function of time.

## Results

The metastatic potential of the MTLn3 and MTC cell lines has been characterized previously (13, 14). MTLn3 cells are highly metastatic and are very plastic in their motility, *i.e.*, they do not exhibit a stable head-to-tail axis and can rapidly convert the tail into a leading edge (3, 4). They contain less F-actin in the leading edge than MTC cells. MTC cells are nonmetastatic and have a pronounced, relatively stable leading edge containing a large amount of F-actin in comparison to MTLn3 cells (15).

*In situ* hybridization was used to determine the distribution of β-actin mRNA in starved MTLn3 cells and in serum-stimulated MTLn3 cells (Fig. 1*A*). These cells have a broad and thin actin filament-containing lamellipod when stimulated with either serum or EGF (15, 17). In MTLn3 cells growing in all conditions [starved (Fig. 1*A*, *1* and *2*), serum-stimulated cells (Fig. 1*A*, *3–8*), and cells grown in serum continuously (data not shown)], β-actin mRNA showed a diffuse cytoplasmic and perinuclear distribution. In MTC cells growing in serum, β-actin mRNA was distributed in the perinuclear area of the cells and in the leading edge of lamellipods (Fig 1*B*, *1* and *2*). The pattern of mRNA localization was reminiscent of that found in Swiss 3T3 fibroblasts (7) and endothelial cells (9). In serum-starved MTC cells, mRNA became diffusely distributed, with greatly attenuated signal in peripheral regions (Fig. 1*B*, *3* and *4*). Upon stimulation with serum (3 min in Fig. 1*B*, *5–8*), β-actin mRNA reappears in the leading edge. All images in Fig. 1 were deconvolved (the thickness of each optical section = 0.3 μm) so that all effects of cell thickness on signal intensity were excluded. *In situ* hybridization of MTC cells with

oligonucleotide probes recognizing tubulin or lacZ mRNAs showed diffuse and perinuclear staining, and no signal was found in the leading edge (data not shown). This confirms the specificity of the localization of β-actin mRNA in the leading edge of MTC cells.

The motility of these two cell lines was analyzed using DIAS software. MTLn3 cells migrated with significantly shorter net and total paths and had significantly lower speed, directionality, and persistence of movement in comparison with MTC cells (Table 1). In Fig. 2, perimeter and centroid plots are shown for MTLn3 (Fig. 2, *A* and *B*) and MTC (Fig. 2, *C* and *D*) cells. MTC centroid and perimeter plots indicate rectilinear movement in contrast to the plots of MTLn3 cells, which indicate random walking. Therefore, MTC cells showed much more polarized locomotion in comparison with MTLn3 cells.

To determine the polarity of MTC and MTLn3 cells *in vivo*, live primary tumors composed of cells labeled with green fluorescent protein were imaged as described previously (2) and compared to conventional H&E-stained paraffin sections of primary MTC and MTLn3 tumors (Fig. 3). By conventional histopathology, both MTC and MTLn3 tumors are poorly differentiated and are composed of cells that form no architectural structures, reminiscent of their cell type of origin, the breast duct epithelial cell. Similarly, the nuclear grade in both tumors, another common benchmark in histopathological evaluation, is comparable. In each, nucleoli are evident, even prominent (Fig. 3, *C* and *D*).

The difference in the appearance of these tumors, both *in vivo* and on histological section, is in the geometry of cell organization and cell-cell contacts. In the MTC tumors, cells appear to be oriented one to another, forming a cohesive sheet that resembles a linear alignment in the section (Fig. 3*C*). This alignment is evident in the *in vivo* images (Fig. 3*A*). In MTLn3 tumors, by contrast, cells appear rounded, noncohesive, and unrelated. Their orientation to one another is the same, regardless of viewing orientation. *In vivo*, the cells appear as independent punctate spheres (Fig. 3, *B* and *D*).

## Discussion

Results obtained in this study indicate that β-actin mRNA is delocalized in MTLn3 cells in comparison with MTC cells, and this delocalization of mRNA correlates with the unpolarized movement and high metastatic potential of MTLn3 cells. It was shown that experimental delocalization of β-actin mRNA in chicken embryo fibroblasts with antisense oligonucleotides decreases the net velocity of cell motility (6). This suggests that delocalization of β-actin mRNA disrupts the interaction of newly synthesized β-actin with actin-binding proteins that are important for maintaining polarized cell motility.

On the basis of our results, we suggest that the inability of metastatic cells to target β-actin mRNA to the leading edge would increase their plasticity of locomotion by depolarizing the cytoskeleton. This would result in cells with an increased flexibility to respond to chemotactic signals, regardless of the direction of origin. On the other hand, cells that target mRNA to the leading edge would establish an intrinsic polarity that would resist changes in polarization caused by extracellular signals.

Spontaneous delocalization of β-actin mRNA in MTLn3 cells compared to MTC cells could be the result of a disturbance of targeting mechanisms in MTLn3 cells. Bundles of EF1α and F-actin formed *in vitro* have a unique bonding rule that would exclude all other known actin-binding proteins (18). The localization of β-actin mRNA in chicken embryo fibroblasts is dependent on actin filaments (19). Therefore, it was proposed that a specific F-actin-EF1α compartment is formed in cells, and this is the compartment to which β-actin mRNA is targeted and then translated (20, 21). In some cancer cell lines, the EF1α-F-actin compartment could be disturbed, and this could lead to the delocalization of mRNA. In fact, EF1α in MTLn3 cells has a lower affinity for actin filaments compared to MTC cells and fails to localize stably to the leading edge (14). This could disassemble the EF1α-F actin compartment, thereby delocalizing mRNA. Furthermore, it was found that the PTI-1 oncogene is a truncated and mutated EF1α containing the dominant actin-binding site of EF1α (22, 23), suggesting that PTI-1 is a dominant negative inhibitor of the actin binding activity of EF1α. This could cause disassembly of the F-actin-EF1α compartment and induce a delocalized mRNA phenotype, resulting in invasive cells.

Further work will be required to test these hypotheses and to determine whether mRNA localization correlates with metastatic potential in a variety of tumors.

## Acknowledgments

We thank Michael Cammer and Shailesh M. Shenoy (Analytical Imaging Facility, Albert Einstein College of Medicine) for technical help with light microscopy and DIAS, and Steve Braut for probe synthesis.

## References

1. Condeelis, J., Jones, J., and Segall, J. H. Chemotaxis of metastatic tumor cells: clues to mechanisms from the *Dictyostelium* paradigm. Cancer Metastasis Rev., *11:* 55–68, 1992.
2. Farina, K. L., Wyckoff, J. B., Rivera, J., Lee, H., Segall, J. E., Condeelis, J. S., and Jones, J. G. Cell motility of tumor cells visualized in living intact primary tumors using green fluorescent protein. Cancer Res., *58:* 2528–2532, 1998.
3. Bailly, M., Yan, L., Whitesides, G., Condeelis, J. S., and Segall, J. E. Regulation of protrusion shape and adhesion to the substratum during chemotactic responses of mammalian carcinoma cells. Exp. Cell Res., *241:* 285–299, 1998.
4. Chan, A. Y., Raft, S., Bailly, M., Wyckoff, J. B., Segall, J. E., and Condeelis, J. S. EGF stimulates an increase in actin nucleation and filament number at the leading edge of the lamellipod in mammary adenocarcinoma cells. J. Cell Sci., *111:* 199–211, 1998.
5. Lawrence, J. B., and Singer, R. H. Intracellular localization of messenger RNA for cytoskeletal proteins. Cell, *45:* 407–415, 1986.
6. Kislauskis, E. H., Zhu, X., and Singer, R. H. β-Actin messenger RNA localization and protein synthesis augment cell motility. J. Cell Biol., *136:* 1263–1270, 1997.
7. Hill, M. A., Schedlich, L., and Gunning, P. Serum-induced signal transduction determines the peripheral location of β-actin mRNA within the cell. J. Cell Biol., *126:* 1221–1230, 1994.
8. Kislauskis, E. H., Zhu, X., and Singer, R. H. Sequences responsible for intracellular localization of β-actin messenger RNA also affect cell phenotype. J. Cell Biol., *127:* 441–451, 1994.
9. Hoock, T. C., Newcomb, P. M., and Herman, I. M. β-Actin and its mRNA are localized at the plasma membrane and the regions of moving cytoplasm during the cellular response to injury. J. Cell Biol., *112:* 653–664, 1991.
10. Ross, A. F., Oleynikov, Y., Kislauskis, E. H., Taneja, K. L., and Singer, R. H. Characterization of a β-actin mRNA zipcode-binding protein. Mol. Cell. Biol., *17:* 2158–2165, 1997.
11. Shuster, C. B., and Herman, I. M. Indirect association of ezrin with F-actin: isoform specificity and calcium sensitivity. J. Cell Biol., *128:* 837–848, 1995.
12. Shuster, C. B., Lin, A. Y., Nayak, R., and Herman, I. M. β-CAP73: a novel β-actin-specific binding protein. Cell Motil. Cytoskeleton, *35:* 175–187, 1996.
13. Neri, A., Welch, D., Kawaguchi, T., and Nicolson, G. L. Development and biologic properties of malignant cell sublines and clones of a spontaneously metastasizing rat mammary adenocarcinoma. J. Natl. Cancer Inst., *68:* 507–517, 1982.
14. Edmonds, B. T., Wyckoff, J., Yeung, Y., Wang, Y., Stanley, R. E., Jones, J., Segall, J., and Condeelis, J. Elongation factor-1α is an overexpressed actin-binding protein in metastatic rat mammary adenocarcinoma. J. Cell Sci., *109:* 2705–2714, 1996.
15. Wyckoff, J., Insel, L., Khazaie, K., Lichtner, R. B., Condeelis, J., and Segall, J. Suppression of ruffling by the EGF receptor in chemotactic cells. Exp. Cell Res., *242:* 100–109, 1998.
16. Soll, D. R. The use of computers in understanding how animal cells crawl. Int. Rev. Cytol., *163:* 43–104, 1995.
17. Segall, J. E., Tyerech, S., Boselli, L., Masseling, S., Helft, J., Chan, A., Jones, J., and Condeelis, J. EGF stimulates lamellipod extention in metastatic mammary adenocarcinoma cells by an actin-dependent mechanism. Clin. Exp. Metastasis, *14:* 61–72, 1996.
18. Owen, C., Derosier, D., and Condeelis, J. Actin cross-linking protein EF-1α of *Dictyostelium discoideum* has a unique bonding rule that allows square-packed bundles. J. Struct. Biol., *109:* 248–254, 1992.
19. Sundell, C., and Singer, R. H. Requirement of microfilaments in sorting of actin messenger RNA. Science (Washington DC), *253:* 1275–1277, 1991.
20. Liu, G., Edmonds, B., and Condeelis, J. pH, EF-1α and the cytoskeleton. Trends Cell Biol., *6:* 168–171, 1996.
21. Liu, G., Tang, J., Edmonds, B. T., Murray, J., Levin, S., and Condeelis, J. F-actin sequesters elongation factor 1α from interaction with aminoacyl-tRNA in a pH-dependent reaction. J. Cell Biol., *135:* 953–963, 1996.
22. Shen, R., Su, Z-Z., Olsson, C. A., and Fisher, P. Identification of the human prostatic carcinoma oncogene PTI-1 by rapid expression cloning and differential RNA display. Proc. Natl. Acad. Sci. USA, *92:* 6778–6782, 1995.
23. Su, Z-Z., Goldstein, N. I., and Fisher, P. B. Antisense inhibition of the PTI-1 oncogene reverses cancer phenotypes. Proc. Natl. Acad. Sci. USA, *95:* 1764–1769, 1998.